

ORIGINAL RESEARCH ARTICLE

Passivation effect analysis of passivation layer based on data analysis

Peng Li*, Jun Wang

Shanghai DianJi University, Shanghai 20240, China. E-mail: 1204405633@qq.com

ABSTRACT

The passivation layer of solar cells directly affects the performance of solar cells. The fixed charge density and defect density at the interface of the passivation layer are the key parameters to analyze the passivation effect. Through establishing the MOS model to simulate the capacitance-voltage ($C-V$) curve of the passivation layer, and using the function to express the simulation curve, this paper establishes the function-based database. The $C-V$ curve obtained from the experiment is compared with the database to find the corresponding function of the experimental data. The passivation parameters N_f and D_{it} are extracted for analyzing the passivation effect of the passivation layer.

Keywords: MOS Model; Database; Defect Density; Fixed Charge Density

ARTICLE INFO

Received: 27 June 2021
Accepted: 25 July 2021
Available online: 7 August 2021

COPYRIGHT

Copyright © 2021 Peng Li, *et al.*
EnPress Publisher LLC. This work is licensed
under the Creative Commons Attribution-
NonCommercial 4.0 International License
(CC BY-NC 4.0).
<https://creativecommons.org/licenses/by-nc/4.0/>

1. Introduction

The problem of energy crisis is becoming more and more prominent at present. People's energy demand is gradually increasing, but the storage of fossil fuels is gradually decreasing, and people's research on new energy is accelerating. As a new type of energy, solar energy has become a hot researching point for its advantages such as its safety and reliability, no noise, no pollution, being available everywhere, no geographical restrictions, no fuel consumption, no mechanical rotating parts, low failure rate, simple maintenance, being unattended, short construction cycle, being easily combined with buildings^[1]. Gas silicon material has become the most ideal material for making solar cells because of its moderate band gap, high photoelectric conversion efficiency, no pollution to the environment, stable performance, easy industrial production and rich resources. Among them, crystalline silicon solar cells are the most efficient, the most widely used solar cells with the most mature technology. In order to save silicon materials and reduce the cost, manufacturers try to reduce the battery thickness. With the increase of the aspect ratio, the passivation problem of the cell surface is becoming more and more prominent, making the judgment and analysis of battery surface passivation effect important.

There are two kinds of cell surface passivation: chemical passivation and field effect passivation. The former usually combines hydrogen atoms or atoms in semiconductor films with uncoordinated atoms on the surface of silicon layer, so as to reduce the interface defect density and improve the photoelectric conversion efficiency of the cell; the latter reduces the concentration of electrons or holes at the silicon

wafer interface through the electric field of the surface charge, so as to achieve the passivation effect^[2]. Both kinds of surface passivation can be measured through the interface defect densities D_{it} and the fixed charge density N_f respectively.

This paper mainly studies the deposition of Al_2O_3 by atomic layer deposition (ALD), establishes an effective MOS model to simulate the $C-V$ characteristic diagram of the MOS structure, and then analyzes the passivation effect of the passivation layer by analyzing the $C-V$ characteristic diagram. The specific passivation effect is measured by the fixed charge density N_f and the interface defect density D_{it} . Both will change the capacitance of the MOS structure. Only one characteristic curve can not accurately express the passivation effect, and most of the existing references use simplified calculation to obtain these two parameters, so its accuracy can not be guaranteed. Therefore, this paper establishes an MOS model to simulate the $C-V$ curve of the MOS structure to obtain these two parameters. Based on the MOS structure, the passivation database of the passivation layer is established; the function corresponding to the experimental data is obtained by comparing the experimental data with the database; the function passivation parameters are extracted to analyze the passivation effect of the passivation layer.

2. Establishment of the MOS model

In order to better study the passivation performance of the crystalline silicon passivation layer, a metal oxide model is established to extract the fixed charge density N_f and defect density D_{it} at the interface between oxide and silicon. These two factors are reflected by the $C-V$ characteristic test chart. First, input the N_f and D_{it} of the original interface state, $C-V$ test results, oxide and silicon parameters, set the original value of gate voltage V_G , and calculate the interface potential Ψ_s at this time; then calculate the silicon surface capacitance C_s and the total capacitance C . Thus, the correlation between the $C-V$ characteristic diagram of the model and the experiment is compared. If the correlation is not good, change the gate voltages V_G , N_f and D_{it} until the correlation

meets the requirements; then output N_f and D_{it} at this time. The specific process is shown in **Figure 1**^[3-5].

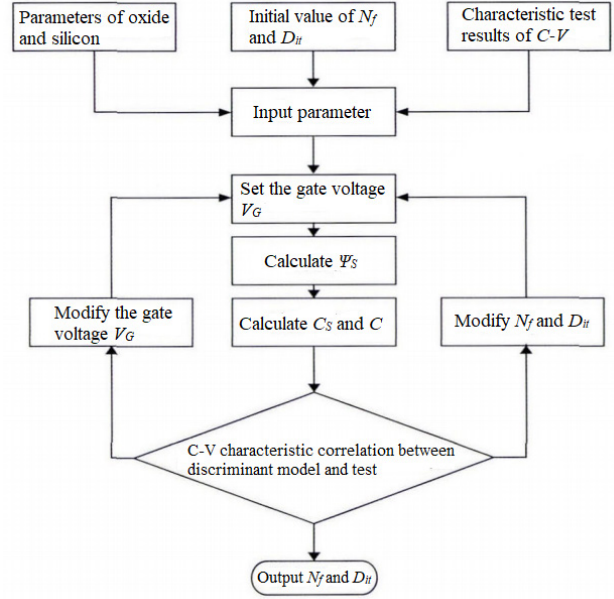


Figure 1. Algorithm flow of fixed charge density N_f and interface defect density D_{it} .

The calculation formula of interface potential Ψ_s is:

$$Q_G(\Psi_s) + Q_f + Q_{it}(\Psi_s) + Q_{Si(acc)}(\Psi_s) = 0 \quad (1)$$

In the formula, Q_G is the gate charge; Q_f is the fixed charge of oxide layer; Q_{it} is the fixed charge at the interface between oxide and silicon; $Q_{Si(acc)}$ is the fixed charge of the silicon layer under standard conditions.

According to the original experimental data of interface^[6,7], the distribution of defect density can be obtained; the formula to calculate D_{it} can be obtained through the algorithm flow in **Figure 1**. Formula (2) can fit the discrete distribution data of defect density to form a curve.

$$D_{it}(E) = \begin{cases} K \left[D_{it,m} + D_{ov} \exp\left(\frac{E_v - E_{it}}{E_{ov}}\right) \right], & \left(E_v \leq E_{it} \leq E_v + \frac{E_g}{2} \right) \\ K \left[D_{it,m} + D_{oc} \exp\left(\frac{E_{it} - E_c}{E_{oc}}\right) \right], & \left(E_v + \frac{E_g}{2} \leq E_{it} \leq E_c \right) \end{cases} \quad (2)$$

In the formula, K is the equilibrium constant, generally taken as 1; E is the battery energy level; E_v and E_c are the upper and lower energy level limits of battery energy level respectively; E_g is the energy

level bandwidth of the battery, $E_g = E_c - E_v$; E_{it} is the energy level of crystalline silicon; $D_{it,m}$ is the defect density at the energy level division; D_{ov} and D_{oc} are respectively defect density at energy levels E_v and E_c .

To establish a model to simulate the C - V characteristic curve of the battery, it is necessary to further calculate other variables and finally integrate them into function of N_f and D_{it} . First, the total capacitance C of the battery MOS structure can be calculated by formula (3)^[8]:

$$C = \left(\frac{1}{C_s} + \frac{1}{C_{ox}} \right)^{-1} \quad (3)$$

In the formula, C_{ox} is the electrical capacity per unit area on the dielectric.

C_{ox} can be figured out with formula (4):

$$C_{ox} = \frac{\epsilon_{ox}}{d_{ox}} = \frac{t_{ox} C_{acc}}{A} \cdot \frac{1}{d_{ox}} \quad (4)$$

In the formula, d_{ox} is the thickness of the dielectric; t_{ox} is the thickness of the oxide layer Al_2O_3 ; A is the area of the MOS layer; C_{acc} is the test capacitance under standard conditions; ϵ_{ox} is the dielectric constant per unit area of the dielectric.

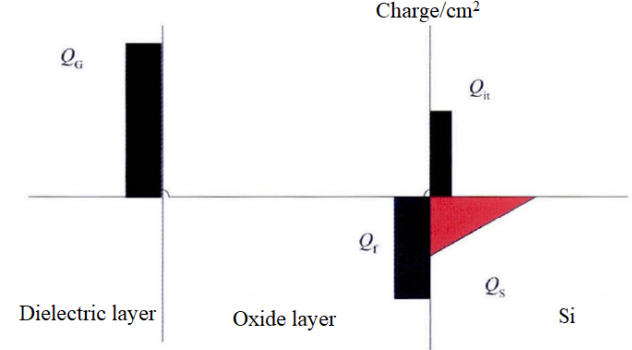
In addition, C_s is obtained on the high frequency C - V characteristic diagram, and its calculation formula is:

$$\begin{aligned} C_s &= \frac{dQ_{S(majority, dopant)}}{d\psi_s} \\ &= q \sqrt{\frac{\epsilon_{si} \epsilon_0 N_D}{2kT}} \cdot \left[\left(e^{\frac{q\psi_s}{kT}} - \frac{q\psi_s}{kT} - 1 \right) + \frac{n_1^2}{N_D^2} \left(\frac{q\psi_s}{kT} \right) \right]^{-\frac{1}{2}} \\ &\quad \left[\left(e^{\frac{q\psi_s}{kT}} - 1 \right) + \frac{n_1^2}{N_D^2} \right] \end{aligned} \quad (5)$$

In the formula, $Q_{S(majority, dopant)}$ is the charge density of dopants and most carriers on the surface of semiconductor silicon; ϵ_{si} and ϵ_0 are the permittivity of silicon and dielectric respectively; k is Boltzmann constant; T is the thermodynamic temperature; q is the electric quantity per unit charge; N_D is the electric ion concentration of dopant; n_1 is the free electron

density in doped crystalline silicon.

The charge distribution of the MOS structure is shown in **Figure 2**.



The formulas for calculating ψ_s can be found in references^[7,9], which can be calculated by formulas (6) to (14).

$$Q_{si} + Q_f + Q_G + Q_{it} = 0 \quad (6)$$

$$Q_G = \frac{-1}{d_{ox}} \left[Q_f \frac{d_f}{2} + \epsilon_{ox} (\psi_s - V_G) \right] \quad (7)$$

$$\begin{aligned} Q_{si} &= \pm \epsilon_{si} \epsilon_0 \cdot E_{si} = \pm \sqrt{2kTN_D \epsilon_{si} \epsilon_0} \cdot \\ &\quad \left[\left(e^{\frac{q\psi_s}{kT}} - \frac{q\psi_s}{kT} - 1 \right) + \frac{n_1^2}{N_D^2} \left(e^{-\frac{q\psi_s}{kT}} + \frac{q\psi_s}{kT} - 1 \right) \right]^{\frac{1}{2}} \end{aligned} \quad (8)$$

$$Q_{it} = -q \int_{E_i}^{E_c} D_{it,a}(E) f_a(E) dE + q \int_{E_v}^{E_i} D_{it,d}(E) f_d(E) dE \quad (9)$$

$$f_a(E) = \frac{\sigma_p p_1 + \sigma_n n_s}{\sigma_p (p_s + p_1) + \sigma_n (n_s + n_1)} \quad (10)$$

$$f_d(E) = \frac{\sigma_p p_s + \sigma_n n_1}{\sigma_p (p_s + p_1) + \sigma_n (n_s + n_1)} \quad (11)$$

$$n_s = N_D e^{\frac{q\psi_s}{kT}}, \quad p_s = \frac{n_i^2}{N_D} e^{\frac{q\psi_s}{kT}} \quad (12)$$

$$n_1 = n_i e^{\frac{E_1 - E_i}{kT}}, \quad p_1 = n_i e^{-\frac{E_1 - E_i}{kT}} \quad (13)$$

$$Q_f = qN_f \quad (14)$$

In the formulas, n_s and p_s represent carrier density of the silicon surface's free charge under the structure of type n and type p; σ_n is the electron trapping interface of defects ON the surface; σ_p is the defect hole trapping interface on the surface; p_1 is the hole density in the crystalline silicon after doping; n_i is the intrinsic carrier concentration of semiconductor; E_{si} is the electric field strength of silicon layer; d_f is the thickness of oxide layer; $f_a(E)$ and $f_d(E)$ are respectively composite probability of acceptor and donor interface; $D_{it,a}$ and $D_{it,d}$ are respectively defect density of acceptor and donor interface; E_i and E_t are respectively energy level midpoint and target energy level; Q_{si} is the charge density of semiconductor silicon's surface.

The positive and negative of Q_{si} is determined by the gate voltage V_G and the flat band voltage V_{FB} . When $V_G \geq V_{FB}$, Q_{si} is negative; when $V_G \leq V_{FB}$, Q_{si} is positive.

The flat band voltage V_{FB} can be calculated by equation (15):

$$V_{FB} = \Phi_{MS} + \frac{Q_f d_f}{2\epsilon_0 \epsilon_{OX}} - \frac{Q_f d_{OX}}{\epsilon_0 \epsilon_{OX}} + \frac{Q_{it} d_{it}}{2\epsilon_0 \epsilon_{OX}} - \frac{Q_{it} d_{OX}}{\epsilon_0 \epsilon_{OX}} \quad (15)$$

In the formula, Φ_{MS} is the metal effective function in the MOS structure, which is different from metal electron affinity and semiconductor Fermi level; d_{OX} is the dielectric thickness; d_{it} is the charge thickness of the contact surface between dielectric and silicon.

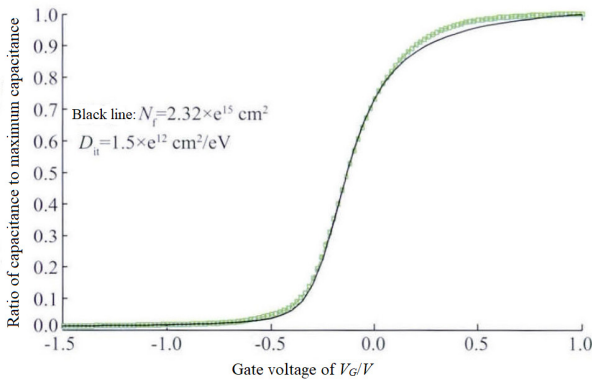


Figure 3. Fitting comparison between simulation curve and experimental data.

Figure 3 shows the final model effect, in which the black line is the fitting curve of the established MOS model to the experimental data, so as to observe whether the fitting effect meets the require-

ments.

3. Big data algorithm

The establishment of large database is based on the above model. When analyzing the passivation performance of on-site solar cells, it is mainly to calculate its fixed charge density N_f and interface defect density D_{it} . The passivation effect of this battery is analyzed through these two data^[10]. Firstly, a function with good correlation is established through the model to fit the C - V characteristic diagram of the battery, and then the two parameters N_f and D_{it} are changed to establish a model about N_f and D_{it} . See equation (16):

$$\begin{cases} f(N_1, D_1) \\ f(N_2, D_2) \\ \vdots \\ f(N_{n-1}, D_{n-1}) \\ f(N_n, D_n) \end{cases} \quad (16)$$

Then, find multiple key points on the battery C - V characteristics, and their coordinates are (x_1, y_1) , (x_2, y_2) , (x_3, y_3) , ..., (x_i, y_i) . Substitute these coordinates into the function group, so as to obtain a set of function sequence, as shown in equation (17):

$$\begin{cases} f_1(N_1, D_1) & f_2(N_1, D_1) & f_3(N_1, D_1) & \cdots & f_i(N_1, D_1) \\ f_1(N_2, D_2) & f_2(N_2, D_2) & f_3(N_2, D_2) & \cdots & f_i(N_2, D_2) \\ \vdots & \vdots & \vdots & & \vdots \\ f_1(N_{n-1}, D_{n-1}) & f_2(N_{n-1}, D_{n-1}) & f_3(N_{n-1}, D_{n-1}) & \cdots & f_i(N_{n-1}, D_{n-1}) \\ f_1(N_n, D_n) & f_2(N_n, D_n) & f_3(N_n, D_n) & \cdots & f_i(N_n, D_n) \end{cases} \quad (17)$$

Subtract the calculated function value from the coordinate value to obtain the error value ϵ of each coordinate point, and sum the absolute values of these error values to obtain formula (18):

$$\begin{cases} \sum |\epsilon_1| + |\epsilon_2| + |\epsilon_3| + \dots + |\epsilon_i| \\ \sum |\epsilon_1| + |\epsilon_2| + |\epsilon_3| + \dots + |\epsilon_i| \\ \vdots \\ \sum |\epsilon_1| + |\epsilon_2| + |\epsilon_3| + \dots + |\epsilon_i| \end{cases} \quad (18)$$

In the formula, $\varepsilon_i = f_i(N, D) - y_i$.

By evaluating the minimum value of equation (18), the function with the minimum error value $f(N_i, D_i)$ can be obtained. This function is the function curve that can be perfectly fitted with the battery. The fixed charge density and interface defect density in this function are the parameters of the actual battery, so that the passivation type and its proportion of the battery can be determined.

4. Analysis of the results

In this paper, we choose the PECVD method to make Al_2O_3 film as the passivation layer of solar cell. Firstly, the fixed parameters are modified according to the experimental data until the MOS model can completely simulate the C - V characteristic curve of the battery; Then, keep other parameters unchanged, change the two parameters of fixed charge density and defect density; as shown in **Figure 3**, set the fixed charge density as $2 \times 10^{16} \text{ m}^{-2}$, assign D_{it} $1 \times 10^{16} - 4 \times 10^{16} \text{ m}^2/\text{V}$ respectively, and bring 0.2 errors into the model formula each time to obtain 16 characteristic curves shown in **Figure 4**.

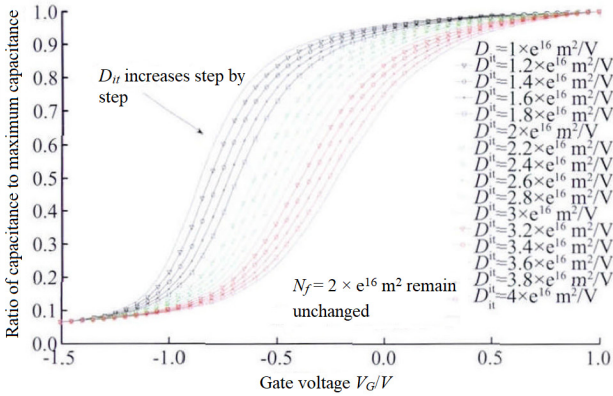


Figure 4. C - V characteristics curve under different D_{it} .

In **Figure 4**, with the increase of defect density, the decline speed of the corresponding characteristic curve decreases and the inclination of the curve decreases, which also means that with the increase of defect density, the corresponding curve has a downward trend.

Figure 5 shows that when the defect density is determined to be $2 \times 10^{16} \text{ m}^2/\text{V}$, change the fixed charge density and assign it to $2 \times 10^{16} - 3.5 \times 10^{16} \text{ m}^{-2}$ respectively, with 0.1 error each time; then bring

it into the model to simulate 16 C - V characteristic curves in the figure, which can be included in the database as data.

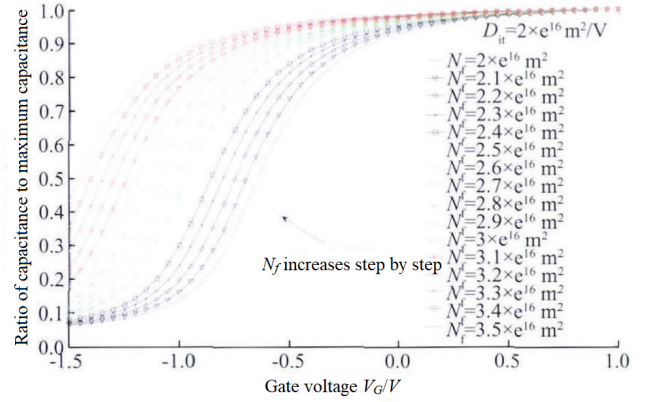


Figure 5. C - V characteristics curve under different N_f .

In **Figure 5**, with the increase of N_f the curve is also moving upward, and the rising rate of the curve is also decreasing. This means that with the increase of N_f , the corresponding curve shows an upward trend, which is just opposite to the effect of defect density.

Figure 6 is a comprehensive diagram of the experimental data obtained from the characteristic measurement of the battery when the passivation times are 40, 80 and 200 respectively. Compare **Figure 6** with **Figures 4** and **5**, and observe the change with the passivation times, what is the change of the parameters of N_f and D_{it} .

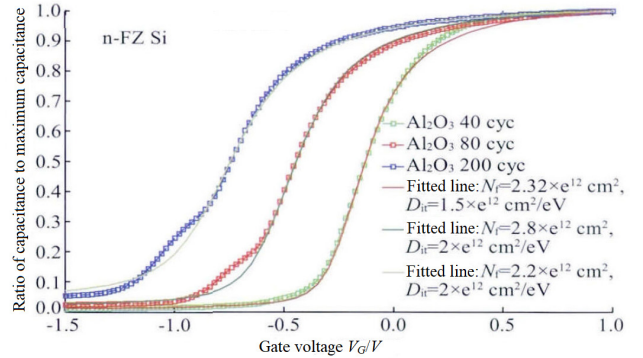


Figure 6. Characteristic curve under different passivation times.

By comparing **Figure 4** to **Figure 6**, it can be found that the value of defect density decreases with the increase of passivation times. This is because with the increase of passivation times, the thickness of passivation medium is also increasing, the defects in the medium layer are also increasing, and the passivation effect is also decreasing; however, the corre-

sponding is the fixed charge density, which increases with the increase of passivation times, which leads to the improvement of battery passivation effect. Therefore, the passivation effect can be analyzed by the proportion of N_f and D_{it} in passivation performance.

5. Conclusions

In this paper, a model to simulate the passivation effect of the MOS structure is built through the calculation equations of various parameters in the battery. The passivation effect of the passivation layer is expressed by curves through the model, and the passivation curve library is established based on the model. The data analysis method is used to compare the passivation curve of the target battery with the curve in the database, and calculate the error value between the curves. The curve in the curve library corresponding to the minimum value is regarded as the simulation curve of the target battery, and the passivation parameters corresponding to the simulation curve are regarded as the experimental data parameters, so as to analyze the passivation effect of the passivation layer.

The curves in the curve library are classified by two parameters. The change of passivation times can be known through curve comparison, which affects the change of passivation parameters in the curve library. In practical application, the target battery can be transformed through the corresponding change trend to meet the requirements. There are many passivation parameters of battery in practice. Other parameters are simplified in this paper, and the parameter of battery thickness is also simplified. However, in practice, the thickness of different batteries under the same conditions is also different. Therefore, if the battery is analyzed for extended passivation, the thickness of battery passivation layer is also a reference parameter that can be extended.

Conflict of interest

The authors declare that they have no conflict of

interest.

References

1. Zheng X. Research on the passivation technology of crystalline silicon solar cell [PhD thesis]. Hangzhou: Zhejiang University.
2. Lang F. Study on passivation properties of Al_2O_3 thin films for n-type solar cells (in Chinese). China High-Tech Enterprises 2016; 34: 28–29.
3. Wang J, Mottaghian SS, Baroughi MF. Passivation properties of atomic-layer-deposited hafnium and aluminum oxides on Si surfaces. IEEE Transactions on Electron Devices 2012; 59(2): 342–348.
4. Budhraj V, Devayajanam S. Effect of SiO_2 passivation on CdTe based solar cells. 2015 IEEE 42nd Photovoltaic Specialist Conference (PVSC); 2015 Jun 14–19; New Orleans. IEEE; 2015. p. 1–3.
5. Xin Z, Dutttagupta S, Tang M, *et al.* An improved methodology for extracting the interface defect density of passivated silicon solar cells. IEEE Journal of Photovoltaics 2016; 6(5): 1080–1089.
6. Fedorenko YG, Truong L, Afhnas'ev VV, *et al.* Energy distribution of the (100)Si/HfO₂ interface states. Applied Physics Letters 2004; 84(23): 4771–4773.
7. Girisch R, Mertens BP, De Keersmaecker RF. Determination of Si-SiO₂/sub 2/interface recombination parameters using a gate-controlled point-junction diode under illumination. IEEE Transactions on Electron Devices 1988; 35(2): 203–222.
8. Schroeder DK. Semiconductor material and device characterization. Wiley 1998; 44(4): 107–108.
9. Aberle AG, Glunz S, Warta W. Impact of illumination level and oxide parameters on Shockley–Read–Hall recombination at Si-SiO₂ interface. Journal of Applied Physics 1992; 71(9): 4422–4431.
10. Van de Loo BWH, Knoop HCM, Dingemans G, *et al.* “Zero-charge” SiO₂/AL₂O₃ stacks for the simultaneous passivation of n⁺ and p⁺ doped silicon surfaces by atomic layer deposition. Solar Energy Materials & Solar Cells 2015; 143: 450–456.